American Mineralogist, Volume 74, pages 812–817, 1989

The hydrous component of sillimanite

ANTON BERAN,* GEORGE R. ROSSMAN
Division of Geological and Planetary Sciences, California Institute of Technology, Pasadena, California 91125, U.S.A.
EDWARD S. GREW
Department of Geological Sciences, University of Maine, Orono, Maine 04469, U.S.A.

ABSTRACT

Polarized infrared spectra of a suite of sillimanite samples from high-grade regionally metamorphosed rocks and associated quartz veins and pegmatites (upper-amphibolite to pyroxene granulite facies), from xenoliths in basaltic rocks, and from alluvial deposits indicate that hydroxyl is the dominant hydrous species bound in sillimanite. Absorption bands at 3556, 3329, 3300, and 3248 cm^{-1} are characteristic of many of the samples. Heating experiments indicate that only above 700 °C is weight loss primarily due to loss of structurally bound OH. Complete dehydration required heating to 1400 °C. The maximum content of bound OH in the sillimanites was 0.02 wt% H_2O equivalent. The intensities of the OH features generally decrease with increasing temperatures estimated for metamorphism, consistent with the expectation that water activities decrease with increasing temperature. However, notable exceptions to this trend suggest that secondary hydration at the unit-cell scale is also a viable explanation for OH incorporation in sillimanite.

INTRODUCTION

Trace amounts of water have been reported in a number of nominally anhydrous minerals, including the Al_2SiO_5 polymorphs. Sillimanite analyses indicate up to 0.72 wt% H_2O (Aramaki and Roy, 1963; Deer et al., 1982; Beran et al., 1983). Hydroxyl absorption bands have been observed in the infrared spectra of the three Al_2SiO_5 minerals (Beran and Zemann, 1969; Wilkins and Sabine, 1973; Beran et al., 1983; Beran and Götzinger, 1987). However, the mechanism by which OH is accommodated in the Al_2SiO_5 structure is not well understood, and the extent of OH incorporation is unknown. Beran et al. (1983) proposed that the hydroxide incorporation in sillimanite was a charge-compensating response to an Al deficiency on the Al(2) site, whereas Hålenius (1979) suggested that $Fe^{2+} + OH^-$ substitution for $Al^{3+} + O^{2-}$ could be a mechanism. Incorporation of even small quantities of water by either mechanism could have substantial effects of Al_2SiO_5 relations analogous to the shifts in the andalusite-sillimanite transition that Kerrick and Speer (1988) attributed to minor amounts of Fe^{3+}.

The objectives of the present study were to determine whether hydroxyl is commonly incorporated in sillimanite from a variety of parageneses, to determine whether the OH content reflects the environment of formation, and to assess the possible effect on Al_2SiO_5 phase relations.

EXPERIMENTAL DETAILS

The sillimanites listed in Table 1 originate from high-grade regionally metamorphosed rocks and associated quartz veins and pegmatites, from xenoliths in basaltic rocks, and from alluvial deposits (Rossman et al., 1982; Beran et al., 1983; Grew and Rossman, 1985). The regional metamorphic sillimanites formed under conditions of the upper-amphibolite facies (sample numbers 6(?), 7, 8, 9, 10, 11, 13, and 27), hornblende granulite facies (1, 2, 4, and 29) and pyroxene granulite facies (12, 25, and 30; Grew, 1980, 1982; Lal et al., 1987). The conditions for sample 27 were deduced from Thompson (1979) and Crawford and Mark (1982, Fig. 2). Sample 6, which Hålenius (1979) reported to be from "Brevig, Norway" (an old spelling of Brevik, H. Annersten, personal communication, 1988) is tentatively included with the amphibolite-facies group. The sample was most likely collected in the Kongsberg-Bamble area, a dominantly amphibolite-facies complex where metamorphic grade locally reaches the granulite facies (e.g., Barth and Reitan, 1963; Touret, 1971). Annersten (personal communication, 1988) has reported that quartz and cordierite, but not K-feldspar, accompanies the sillimanite (cf. Hålenius, 1979). Sample 30 is included with the pyroxene granulite–facies rocks because this sillimanite-bearing rock is associated with sapphirine-quartz rocks.

Metamorphic temperatures for the Antarctic pyroxene granulite facies (Napier Complex) are estimated to be 800–900 °C (sample 12) and at least 900 °C (sample 25) with $P_{H_2O} \ll P_{total}$ (e.g., Grew, 1980, 1981a; Sheraton et al., 1987) and for the Indian (Paderu) terrane, 800–900 °C (sample 30) (Grew, 1982; Lal et al., 1987). Temperatures

* Permanent address: Institut für Mineralogie und Kristallographie, Universität Wien, Dr. Karl Lueger-Ring 1, A-1010 Vienna, Austria.

0003–004X/89/0708–0812$02.00

TABLE 1. Sillimanite infrared absorbance in the OH region

No.*	Sample	Locality	Origin†	Band position (cm^{-1})				
				3556	3329	3300	3248	3205
1	GRR 273	Reinbolt Hills, Antarctica	HG	0.127	0.037	0.060	0.184	0.000
2	GRR 439	Molodezhnaya Station, Antarctica	HG	0.096	0.105	0.105	0.166	0.000
3	GRR 385	Kilbourne Hole, New Mexico	X	0.096	0.000	0.000	0.000	0.000
4	GRR 380	Benson Mines, New York	HG	0.140	0.000	0.089	0.242	0.076
6‡	GRR 1585	Brevik, Norway	UA	0.056	0.000	0.000	0.000	0.000
7	GRR 384	Willimantic, Connecticut	UA	0.000	0.000	0.000	0.000	0.000
8	GRR 547	Vernon, Connecticut	UA	0.175	0.000	0.197	0.263	0.110
9	GRR 383	Guilford (?), Connecticut	UA	0.112	0.000	0.117	0.166	0.057
10	GRR 450	Oconee County, South Carolina	UA	0.172	0.000	0.215	0.215	0.189
11	GRR 382	Sardinia (?)	?	0.292	0.097	0.248	0.529	0.097
12	GRR 608	"Christmas Point," Antarctica	PG	0.138	0.000	0.000	0.055	0.000
13	GRR 386	Norwich, Connecticut	UA	0.216	0.000	0.216	0.281	0.195
14	GRR 311	Kilbourne Hole, New Mexico	X	0.000	0.000	0.000	0.000	0.000
17	GRR 509	Mogok, Burma	AG	0.275	0.245	0.200	0.300	0.120
19	GRR 306	Bournac, France	X	0.161	0.000	0.117	0.073	0.000
25	GRR 560	Beaver Island, Antarctica	PG	0.000	0.000	0.000	0.000	0.000
26	GRR 1485	Sri Lanka	AG	0.053	0.000	0.000	0.032	0.000
27	AB-Gho	Brandywine Springs, Delaware	UA	0.249	0.111	0.276	0.406	0.087
28	AB-Sm1	Sri Lanka	AG	0.248	0.552	0.505	0.543	0.000
29	GRR 799	Ellammankovilpatti, India	HG	0.283	0.000	0.264	0.377	0.000
30§	GRR 802	Paderu, India	PG	0.0	0.0	0.0	0.0	0.0

Note: All absorbance values (in absorbance per millimeter) are for the $\mathbf{E}\|a$ orientation.

* Numbers 1–19 are the sample numbers of Rossman et al. (1982), which presents a more complete description of these samples. Sample 25 is a fragment of a pale-brown crystal with many inclusions. Sample 26 is a cleavage plate from pale-blue, 2-cm gem-quality crystal. Sample 27 is a fragment of a brown crystal with few fibrous inclusions. It is part of the sample (University of Chicago no. 2261) used by Winter and Ghose (1979). Sample 28 is a pale-brown inclusion-free cleavage plate of a gem-quality crystal. Sample 29 is no. 3083D of Grew and Rossman (1985). Sample 30 is no. E2724 of Grew and Rossman (1985).

† Origins: AG = alluvial deposit presumably from granulite facies; HG = hornblende granulite facies; PG = pyroxene granulite facies; UA = upper-amphibolite grade; X = xenolithic.

‡ The spectrum of sample 6 in the OH region is so dominated by included phases that the tabulated absorbance values are rough estimates. Sample 6 is tentatively included in the upper-amphibolite facies (see text).

§ The detection limit for sample 30, 0.08 per millimeter, is higher than for the others because of the thinness of the sample.

of formation of the hornblende granulite–facies sillimanite range from 700 to 800 °C (*P-T* data for samples 2, 4, and 29 are given in Grew, 1981b; Bohlen et al., 1985; and Grew et al., 1987, respectively) typical of most granulite-facies terranes (Bohlen, 1987). Temperatures for the amphibolite-facies sillimanite probably did not exceed 700 °C, an upper limit of metamorphic temperatures for the amphibolite facies (e.g., Bohlen, 1987). The xenolithic sillimanites (3, 14, and 19) are interpreted to have originated in granulite-facies rocks at depth and to have been subsequently incorporated in basalt and transported to the Earth's surface by explosive volcanic activity. During this transport the xenoliths were subjected to temperatures of near 1000 °C (e.g., Kilbourne Hole, Grew, 1979), partial melting, and quenching. Provenance of the alluvial sillimanites (samples 17, 26, and 28) is unknown; most probably the sillimanite is derived from the granulite-facies rocks exposed in the vicinity of the alluvial deposits.

Infrared spectra were obtained on a Nicolet 60SX Fourier-transform infrared spectrophotometer operating at 2 cm^{-1} resolution. Samples were prepared as doubly polished (010) cleavage plates, 0.5 to 6 mm thick; they were examined through clear areas, as free from inclusions as possible, which varied from 15 × 200 μm to 600 μm in diameter. Heating experiments were conducted in air. A fragment of sample 28 was put in a preheated tube furnace and initially dried for 15 h at 110 °C. It was then removed from the hot zone and immediately allowed to cool in air to room temperature. After it was weighed and its spectrum taken, the process was repeated at a series of specified temperatures (250, 500, 750, and 900 °C). The sample was held at temperature for 1.5 h in each step. An additional heating step at 900 °C for 15 h did not change either the weight or the spectrum. A second fragment heated at 110 °C (15 h), 700 °C (1.5 h), 750 °C (3 hr), and 900 °C (15 h) produced nearly identical results.

RESULTS

Spectroscopic features

A variety of OH-related features appear in the region from 4000 cm^{-1} to 3000 cm^{-1} in all three polarizations of the spectra of sillimanite (e.g., Fig. 1). Although there is much variation among samples involving the minor features, there are four bands prominent in the $\mathbf{E}\|a$ spectrum of many of the samples. They are at 3556, 3329, 3300, and 3248 cm^{-1} (Fig. 2). Additionally, there are weak bands at 3205 and 3163 cm^{-1} in the $\mathbf{E}\|a$ spectra of many samples. There is also a band at 3546 cm^{-1} polarized $\mathbf{E}\|b$. The absolute intensities of these features vary from sample to sample. The feature at about 2663 cm^{-1} is most intense in the $\mathbf{E}\|c$ spectrum, although this direction generally could not be measured with the (010) cleavage slabs

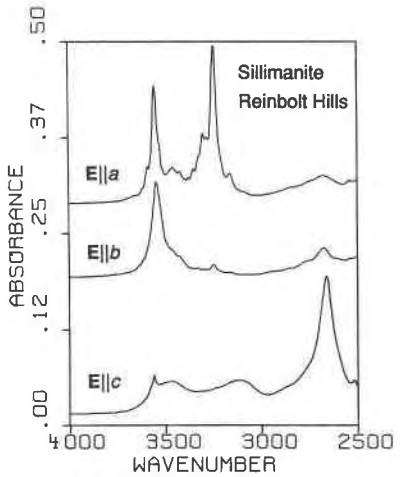

Fig. 1. Infrared spectrum of sillimanite 1 plotted for 1.0-mm thickness in three polarizations.

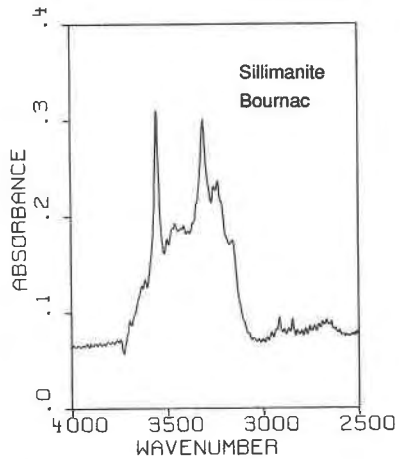

Fig. 3. Infrared spectrum of sillimanite (sample 19) with the second class (type II) of spectrum. Plotted for 1.0-mm thickness; $\mathbf{E} \| a$.

that were used for most of the spectroscopic measurements.

For purposes of classification, many of the spectra can be divided into two groups on the basis of the relative intensity of the bands in the $\mathbf{E} \| a$ polarization. In the first group (type I), there are three prominent bands at 3329, 3300 and 3248 cm^{-1} (Fig. 2, top). Although the relative intensities of the three component bands are variable, one of the bands of this triplet is always more intense than the band at 3556 cm^{-1}. In the second group (type II), the band at 3556 cm^{-1} is the most intense, and the triplet bands are weak or absent (Fig. 3). A few spectra do not fall into either group; the spectra of samples 7, 14 and 25 include none of these bands, although OH features appear at other wavelengths.

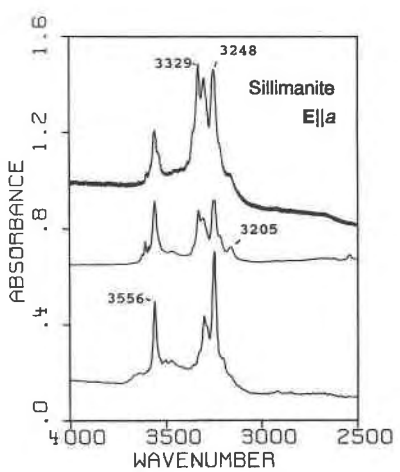

Fig. 2. The infrared spectra of three sillimanites that show the characteristic group of OH bands in the $\mathbf{E} \| a$ polarization. Top: sample 28. Center: sample 17. Bottom: sample 11. All spectra obtained from (010) plates and plotted for 1.0-mm thickness.

Heating experiments

Two fragments (16.4 and 5.2 mg) of sample 28 were subjected to a stepwise heating experiment in which the infrared spectrum was obtained after each step. This sample was chosen because it is free of inclusions, homogeneous in OH content, and large enough for multiple experiments. The fragments were heated at temperatures from 110 to 900 °C. The total weight loss in each case was about 0.07% (Table 2). Although there was weight loss at each step, the OH triplet bands decrease only slightly below 500 °C, indicating that the initial weight loss below 500 °C was not due to the structurally bound OH units. Above 700 °C, the decrease in the infrared intensity at 3329 cm^{-1} and 3248 cm^{-1} correlates with the weight loss. By 900 °C, the OH triplet disappears (Fig. 4). However, between 110 and 500 °C, there is a greater weight loss with a much smaller loss of infrared intensity (Fig. 5). The heating experiments on both fragments of sample 28 produced nearly quantitatively identical results.

Even after heating to 110 °C, there is a broad infrared absorption centered near 3400 cm^{-1} that is lost at higher temperatures. Liquid water absorbs in this spectral region. After the 900 °C treatment, the single OH absorption at 3556 cm^{-1} retains about half of its original intensity, and the spectrum resembles that of the type II samples (e.g., samples 3, 12, 19 and 26). Between 700 and 750 °C, a weak band at 3163 cm^{-1} grows noticeably (Fig. 4). This behavior is reminiscent of the OH band that grows at high temperature in the spectra of topaz owing to site re-equilibration (Aines and Rossman, 1985).

Sample 1 is not fully dehydrated after heating at 1037 °C for 45 h, judging from the presence of a weak, residual absorption at 3556 cm^{-1}. All OH features were absent from its spectrum after it was heated to 1400 °C.

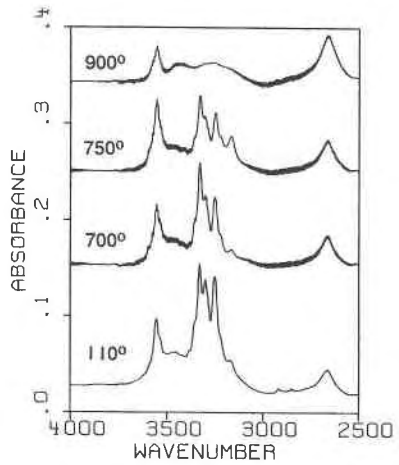

Fig. 4. Infrared spectra of sillimanite (sample 28) after a series of stepwise heating steps showing the loss of OH groups at elevated temperature. Unpolarized spectra presented for a 1.0-mm-thick (010) plate. The spectra were taken after the sample was heated to the indicated temperature and returned to room temperature.

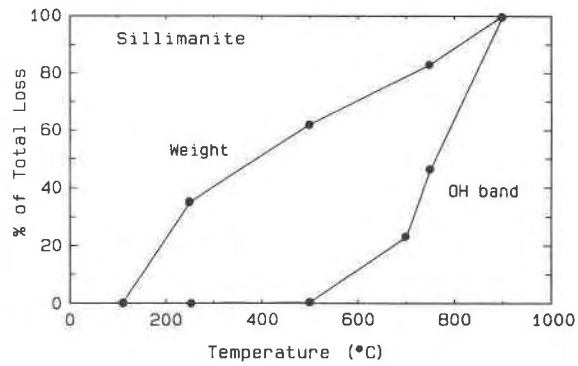

Fig. 5. Stepwise heating equipment (sample 28) showing cumulative weight loss and cumulative loss of intensity of the 3329 cm^{-1} OH band. Much weight loss occurred at lower temperatures before the OH bands began to decrease.

Absolute OH content

The weight loss that accompanies the heating steps between 700 and 900 °C was used to calibrate the sillimanite infrared spectrum under the assumption that the high-temperature weight loss was solely due to the dehydration of bound OH ions. The total weight loss between 700 and 900 °C (0.012 wt%) was associated with the absorbance change in the 3329 cm^{-1} band over the same temperature range (0.160 absorbance units per millimeter of thickness). For the purposes of this calibration, the intensity of the band at 3329 cm^{-1} was used because it is the most prominent band in most sillimanite spectra. Furthermore, its intensity follows the intensities of the other components of the triplet of bands that represent the majority of OH intensity in the sillimanite spectrum.

The total mass of water associated with the decrease in the 3329 cm^{-1} band between 110 and 900 °C was then determined from this calibration. This calculation indicates that only 0.02% OH (expressed as H_2O) is associated with the triplet of bands (Table 2). Although this calibration may underestimate the total OH concentration because it does not account for changes in the minor OH bands, it represents the majority of the OH intensity in the sillimanite spectrum.

Our value of 0.02% H_2O in sample 28 appears to be the maximum for any sillimanite analyzed to date. We doubt that the much higher OH contents previously reported represent bound OH in sillimanite. More likely, these contents include adsorbed water that contributes most of the loss on ignition, as shown by our heating experiments. There is evidence for some water in the IR spectrum of sample 28, possibly as microscopic fluid inclusions, but it is enough to account for only 10% of the low-temperature weight loss. We propose that most of the remaining weight loss occurs from molecular water on the edges of the crystals, probably associated with surface damage and incipient cleavage.

Discussion

The major OH absorption bands in the sillimanite spectra do not correspond to any of the hydrous phases commonly associated with sillimanite. Specifically, OH groups in amphiboles, boehmite, chlorites, diaspore, gibbsite, kaolinite, micas, and pyrophyllite do not absorb in the region of the prominent sillimanite bands. Intensities of these absorption features do not correlate with the abundance of microscopic inclusions that are present in several of the samples. We conclude that many of the hydroxyl absorption features, notably those at 3556, 3329, 3300, 3248, and 3205 cm^{-1}, are characteristic of sillimanite itself and are not due to either hydrous phases included in the sillimanite or hydrous alteration products.

The OH features appear unrelated to the various colored varieties of sillimanite described by Rossman et al. (1982). In particular, they are not correlated with Fe content; both Fe-rich and Fe-poor varieties show OH absorption features. As regards B, our data are limited to three samples (1, 29, and 30; Grew and Rossman, 1985). The spectrum for the sample with the most B (sample

Table 2. The determination of the OH content of two fragments of sillimanite sample 28

	Mass (mg)	
	16.368	5.219
Stepwise heating from 110 to 900 °C		
Weight loss	0.073%	0.077%
Absorbance loss	0.210 mm^{-1}	
Stepwise heating from 700 to 900 °C		
Weight loss	0.016%	0.013%
Absorbance loss	0.160 mm^{-1}	

Note: Total OH loss (expressed as H_2O) from 3329 cm^{-1} band: (0.210 ÷ 0.160) × 0.016% = 0.021%.

30, 0.4% B_2O_3) shows no OH absorption features at all. We thus feel justified in ruling out the substitution $SiO^{2+} = BOH^{2+}$ as a mechanism for hydroxyl incorporation in sillimanite. This conclusion is re-enforced by Grew and Hinthorne's (1983) studies, which indicate that rocks containing B-bearing sillimanite form at high temperatures under low water activities. Thus, we must consider that hydroxyl is incorporated in the sillimanite structure either through a substitution involving Al or Si or by hydrous defects at the unit-cell scale. Other characteristics of the spectral data further support this interpretation.

The energies of several of the OH bands (<3350 cm^{-1}) are lower than the energies commonly observed in silicate minerals that have OH as a part of their normal stoichiometry. The correlation of Nakamoto et al. (1955) between the wavenumber of the OH band and the strength of the hydrogen bond as measured by the O–H···O distance indicates that the O–O distance is less than 2.82 Å, comparable to the O–O distances within the Al octahedra and tetrahedra in the sillimanite structure (Burnham, 1963). Furthermore, the sharpness of the bands suggests that OH rather than H_2O is the vibrating species.

If hydroxyl were incorporated in the structure through the substitution $3(OH)^- + \square = Al^{3+} + 3O^{2-}$ proposed by Beran et al. (1983), we would expect sillimanite water contents to correlate directly with estimated water activities during sillimanite formation. In line with studies of regional metamorphism (e.g., Lamb and Valley, 1988), we presume that the water activities during crystallization would have been greatest for the amphibolite-facies sillimanites and least for the pyroxene granulite–facies sillimanites. Moreover, low contents are predicted for the xenolithic sillimanites, which were subjected first to granulite-facies metamorphism and then heated to high temperatures in a dry environment.

In general, the observed intensities of the OH absorption bands fit these trends. For example, the average intensities of the most intense bands, 3556 cm^{-1} and 3248 cm^{-1}, decrease in the following sequence: amphibolite facies (0.174, 0.266, respectively, from Table 1, excluding sample 6), hornblende granulite facies (0.162, 0.242), xenolith (0.086, 0.024), and pyroxene granulite facies (0.046, 0.018). The differences between successive averages in the sequence are in most cases less than one standard deviation and are thus, strictly speaking, not statistically significant. Nevertheless, the intensities of OH absorption features for sillimanites formed under the driest conditions (pyroxene granulite facies, xenoliths) are significantly less than those for sillimanite formed under wetter conditions. Moreover, the decrease in intensity is more marked for the 3248 cm^{-1} band, because the spectra of the sillimanites from the pyroxene granulite facies and xenoliths are type II or lack absorption features in the 2500 to 4000 cm^{-1} range. By contrast, most of the sillimanites formed under lower-temperature conditions have type I spectra.

Alternatively, secondary hydration could explain the notable exceptions to the observed trends, such as the amphibolite-facies sillimanite that gives a spectrum lacking absorption features in the 4000 to 2500 cm^{-1} range (no. 7) and a relatively hydrated xenolithic sillimanite (no. 19). In this alternative interpretation, the OH absorption features are explained by incipient alteration at the unit-cell scale. For example, water could enter the mineral and be incorporated as submicroscopic lamellae of hydrated aluminosilicate along discrete planes in the sillimanite structure, a situation resembling the occurrence of humite layers in olivine (Kitamura et al., 1987) and the alteration of pyroxene to amphibole in submicroscopic lamellae (Veblen and Buseck, 1981). In contrast to the amphibole lamellae in pyroxene, the lamellae of hydrated aluminosilicate would be so small that OH vibration is controlled by the host sillimanite. The resulting vibrational spectrum would thus be characteristic of sillimanite and unlike known hydrous aluminosilicates such as pyrophyllite or kaolinite. Incorporation of hydroxyl by formation of such a hydrous aluminosilicate would depend on a variety of factors, for example, infiltration of water-rich fluids after crystallization, fracture development during deformation, or retrogression of the high-temperature anhydrous mineral assemblages to lower-temperature assemblages with hydrous phases.

Secondary hydration would be expected to produce variable sillimanite water contents. For example, sillimanite nos. 12 (hydrous) and 25 (anhydrous) both crystallized during an Archean pyroxene granulite–facies event, but only sillimanite no. 12 was subjected to tectonic reactivation and retrogression in the amphibolite facies; sample 25 was not affected (Rossman et al., 1982; Sheraton et al., 1987). Water could have been incorporated into sillimanite no. 12 when associated high-temperature minerals (e.g., surinamite) were replaced by cordierite and biotite formed either during retrograde metamorphism or during a late, water-rich stage of pegmatite crystallization (Grew, 1981a). Relatively high water activities along the retrograde *P-T* path (e.g., no. 29, Grew et al., 1987) or polymetamorphism may account for the OH absorption features in many of the other samples. Wetter conditions at the time of crystallization need not be invoked as the cause. Moreover, the relatively strong absorption of alluvial samples could be attributed to water incorporated during residence in the alluvial deposit rather than during original crystallization.

Clarification of the structural details of water incorporation in sillimanite has important implications for metamorphic petrology. If water is incorporated in sillimanite and other Al_2SiO_5 phases during crystallization through coupled substitutions involving Al and Si, then Al_2SiO_5 phase relations could be significantly affected by fractionation of H_2O among the phases, an effect analogous to that of Fe^{3+} fractionation between andalusite and sillimanite (Kerrick and Speer, 1988). However, if water is incorporated in the Al_2SiO_5 minerals during postmetamorphic processes, the anhydrous compositions would be appropriate for applying theoretical Al_2SiO_5 relations

to experimental results and to rocks, at least as far as the role of water is concerned. Detection of thin, OH-rich lamellae in sillimanite and the other Al_2SiO_5 phases requires careful high-resolution transmission-electron-microscopy studies that are a logical extension of the present study.

Acknowledgments

We acknowledge the following people and institutions for their generosity in providing samples for this study: C. Frondel, Harvard University (samples 9, 13); John S. White, Jr., U.S. National Museum (4, 7, 8, 10, 11); G. E. Harlow, American Museum of Natural History (17); J. Fabriès, Muséum Nationale d'Histoire Naturelle Minéralogie (19); R. I. Gait, Royal Ontario Museum (30); U. Hålenius (6); E. R. Padovani (14); and S. Ghose, University of Washington (27). Portions of this study were funded by the National Science Foundation (U.S.A.) grants EAR-86-18200 and DPP-8613241 and the Austrian Fonds zur Förderung der wissenschaftlichen Forschung (project 3735). Financial support to A. B. by the Fulbright Commission is also acknowledged.

References cited

Aines, R.D., and Rossman, G.R. (1985) The high temperature behavior of trace hydrous components in silicate minerals. American Mineralogist, 70, 1169–1179.

Aramaki, S., and Roy, R. (1963) A new polymorph of Al_2SiO_5 and further studies in the system Al_2O_3-SiO_2-H_2O. American Mineralogist, 48, 1322–1347.

Barth, T.F.W., and Reitan, P.H. (1963) The Precambrian of Norway. In Kalervo Rankama, Ed., The Precambrian, vol. 1, p. 27–80. Interscience-Wiley, New York.

Beran, A., and Götzinger, M.A. (1987) The quantitative IR spectroscopic determination of structural OH groups in kyanites. Mineralogy and Petrology, 36, 41–49.

Beran, A., and Zemann, J. (1969) Messung des Ultrarot-Pleochroismus von Mineralen VIII. Der Pleochroismus der OH-Streckfrequenz in Andalusit. Tschermaks Mineralogie und Petrographie Mitteilungen, 13, 285–292.

Beran, A., Hafner, St., and Zemann, J. (1983) Untersuchungen über den Einbau von Hydroxilgruppen im Edelstein-Sillimanit. Neues Jahrbuch für Mineralogie Monatshefte, 219–226.

Bohlen, S.R. (1987) Pressure-temperature-time paths and a tectonic model for the evolution of granulites. Journal of Geology, 95, 617–632.

Bohlen, S.R., Valley, J.W., and Essene, E.J. (1985) Metamorphism in the Adirondacks. 1. Petrology, pressure, and temperature. Journal of Petrology, 26, 971–992.

Burnham, C.W. (1963) Refinement of the crystal structure of sillimanite. Zeitschrift für Kristallographie, 118, 127–148.

Crawford, M.L., and Mark, L.E. (1982) Evidence from metamorphic rocks for overthrusting, Pennsylvania Piedmont, U.S.A. Canadian Mineralogist, 20, 333–347.

Deer, W.A., Howie, R.A., and Zussman, J. (1982) Rock-forming Minerals: Volume 1A, Orthosilicates. Longman, London.

Grew, E.S. (1979) Al-Si disorder of K-feldspar in crustal xenoliths at Kilbourne Hole, New Mexico. American Mineralogist, 64, 912–916.

——— (1980) Sapphirine + quartz association from Archean rocks in Enderby Land, Antarctica. American Mineralogist, 65, 821–836.

——— (1981a) Surinamite, taaffeite, and beryllian sapphirine from pegmatites in granulite-facies rocks in Casey Bay, Enderby Land, Antarctica. American Mineralogist, 66, 1022–1033.

——— (1981b) Granulite-facies metamorphism at Molodezhnaya Station, East Antarctica. Journal of Petrology, 22, 297–336.

——— (1982) Sapphirine, kornerupine, and sillimanite + orthopyroxene in the charnockitic region of South India. Journal of the Geological Society of India, 23, 469–505.

Grew, E.S., and Hinthorne, J.R. (1983) Boron in sillimanite. Science, 221, 547–549.

Grew, E.S., and Rossman, G.R. (1985) Co-ordination of boron in sillimanite. Mineralogical Magazine, 49, 132–135.

Grew, E.S., Abraham, K., and Medenbach, O. (1987) Ti-poor hoegbomite in kornerupine-cordierite-sillimanite rocks from Ellammankovilpatti, Tamil Nadu, India. Contributions to Mineralogy and Petrology, 95, 21–31.

Hålenius, Ulf. (1979) State and location of iron in sillimanite. Neues Jahrbuch für Mineralogie Monatshefte, 165–174.

Kerrick, D.M., and Speer, J.A. (1988) The role of minor element solid solution on the andalusite-sillimanite equilibrium in metapelites and peraluminous granitoids. American Journal of Science, 288, 152–192.

Kitamura, M., Kondoh, S., Morimoto, N., Miller, G.H., Rossman, G.R., and Putnis, A. (1987) Planar OH-bearing defects in mantle olivine. Nature, 328, 143–145.

Lal, R.K., Ackermand, D., and Upadhyay, H. (1987) *P-T-X* relationships deduced from corona textures in sapphirine-spinel-quartz assemblages from Paderu, southern India. Journal of Petrology, 28, 1139–1168.

Lamb, W.M., and Valley, J.W. (1988) Granulite facies amphibole and biotite equilibria, and calculated peak-metamorphic water activities. Contributions to Mineralogy and Petrology, 100, 349–360.

Nakamoto, K., Margoshes, M., and Rundle, R.E. (1955) Stretching frequencies as a function of distances in hydrogen bonds. Journal of the American Chemical Society, 77, 6480–6488.

Rossman, G.R., Grew, E.S., and Dollase, W.A. (1982) The colors of sillimanite. American Mineralogist, 67, 749–761.

Sheraton, J.W., Tingey, R.J., Black, L.P., Offe, L.A., and Ellis, D.J. (1987) Geology of an unusual Precambrian high-grade metamorphic terrane—Enderby Land and western Kemp Land, Antarctica. Australian Bureau of Mineral Resources Bulletin 223.

Thompson, A.M. (1979) A summary of the geology of the Piedmont in Delaware. Transactions of the Delaware Academy of Science, 7, 115–125.

Touret, Jacques. (1971) Le faciés granulite en Norvége mèridionale. 1. Les associations minéralogiques. Lithos, 4, 239–249.

Veblen, D.R., and Buseck, P.R. (1981) Hydrous pyriboles and sheet silicates in pyroxenes and uralites: Intergrowth microstructures and reaction mechanisms. American Mineralogist, 66, 1107–1134.

Wilkins, R.W.T., and Sabine, W. (1973) Water content of some nominally anhydrous silicates. American Mineralogist, 58, 508–516.

Winter, J.K., and Ghose, S. (1979) Thermal expansion and high-temperature crystal chemistry of the Al_2SiO_5 polymorphs. American Mineralogist, 64, 573–586.

Manuscript received August 12, 1988
Manuscript accepted March 21, 1989